

# Effects of Continuity Plate and Transverse Reinforcement on Cyclic Behavior of SRC Moment Connections

Chung-Che Chou<sup>1</sup> and Chia-Ming Uang<sup>2</sup>

**Abstract:** Two exterior moment connections with a steel-encased reinforced concrete (SRC) column and a steel beam were tested to evaluate the cyclic performance. Continuity plates were eliminated in the first specimen, and about 60% of the transverse reinforcement as specified in the ACI 318 was used in the connection region. Two steel doubler plates offsetting from the column web were used to enhance the shear resistance of the connection. The second specimen used a steel jacket to confine the concrete in the connection region and continuity plates were extended from the steel column to the steel jacket to mobilize the shear resistance of the latter; no transverse reinforcement was used. Full-scale test results showed that both specimens were able to reach an interstory drift ratio in excess of 4%. An analytical model was developed for the concrete shear force transfer mechanism in the connection of the second specimen. This study showed that: (1) using either doubler plates or jacket plates was effective to enhance the shear capacity in the connection, (2) concrete shear resistance degraded before the maximum applied load was reached in the first specimen, (3) the concrete was mobilized to resist shear in the second specimen, and (4) transverse reinforcement as required by the ACI 318 (1995) can be relaxed as long as another shear-resisting mechanism such as doubler plates or jacket plates is provided.

**DOI:** 10.1061/(ASCE)0733-9445(2007)133:1(96)

**CE Database subject headings:** Connections; Reinforcement; Steel beams; Concrete, reinforced; Concrete columns.

## Introduction

Most of the recent research on composite special moment frames has been focused on reinforced concrete steel (RCS) system with reinforced concrete columns and steel beams. Different connection details have been studied in both the United States (Sheikh 1987; Deierlein 1988; Kanno 1993) and Japan (Sakaguchi et al. 1988; Izaki et al. 1988; Kuramoto 1996). These research efforts were intended to develop connection details that can efficiently transfer the steel beam forces to reinforced concrete columns. Failure modes and force transfer mechanisms in the RCS connections were presented. Design equations for the ultimate shear strength of the RCS connections were also developed (AIJ 1994; ASCE Task Committee 1994).

The connections investigated in this study are composed of a steel-encased reinforced concrete (SRC) column and a steel beam. For the SRC connection, a steel wide flange column, encased in reinforced concrete, is continuous through the connection and is welded to the steel beams. However, a steel beam is continuous through the RCS connection. Thus, the concrete shear resistance in the SRC connection is mainly provided by the concrete strut

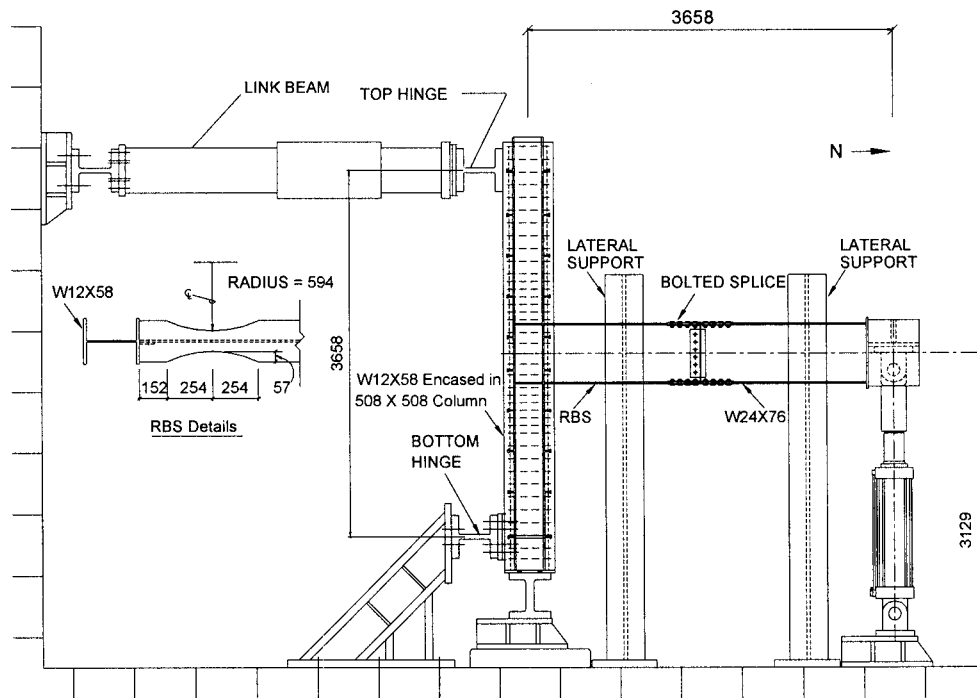
within the steel column flange, and that in the RCS connection is mobilized by the face bearing plates in the steel beams (Deierlein 1988). Research on similar types of SRC connections has been conducted in Japan. Wakabayashi et al. (1973) tested 12 interior moment connection specimens, which were composed of either an SRC column or a reinforced concrete column with SRC beams. When an SRC column was used, the steel beam, which was encased in concrete, was continuous through the connection. The steel column was interrupted and welded to the steel beam. No transverse reinforcement was provided in the connection. Each specimen was designed to fail, in either flexure in the column or shear in the connection. It was reported that longitudinal reinforcement buckled in the connection region for some specimens. Three specimens failed in shear in the connection, which was accompanied by yielding in the steel beam panel zone, and the maximum concrete shear strength reached  $0.5f'_c$ .

Minami and Nishimura (1980) tested 30 beam-column subassemblages to evaluate the shear behavior of interior, exterior, and corner SRC moment connections. The specimens were composed of a same-size SRC column, with an SRC beam of varying width. Continuity plates were provided in the panel zone, but no transverse reinforcement was used in the connection. The ratio of SRC beam width to SRC column width was reported to be an important factor for the ultimate shear strength of the concrete; test results showed that the ultimate shear strengths were in the range of  $(0.2-0.45)f'_c$ ,  $(0.13-0.26)f'_c$ , and  $(0.12-0.24)f'_c$  for interior, exterior, and corner connections, respectively. The study also led to the following conclusions: (1) the ultimate shear strength of the steel column web can be developed; (2) the ultimate shear strength of the concrete in the exterior and corner connections is much smaller than that in the interior connection; (3) the ultimate shear strength of the concrete in the connection increases with the ratio of the SRC beam width to the SRC column width; and (4)

<sup>1</sup>Assistant Professor, Dept. of Civil Engineering, National Chiao Tung Univ., 1001 Ta-hsueh Road, Hsinchu 300, Taiwan (corresponding author). E-mail: chchou@mail.nctu.edu.tw

<sup>2</sup>Professor, Dept. of Structural Engineering, Univ. of California, San Diego, La Jolla, CA 92093. E-mail: cmu@ucsd.edu

Note. Associate Editor: Sherif El-Tawil. Discussion open until June 1, 2007. Separate discussions must be submitted for individual papers. To extend the closing date by one month, a written request must be filed with the ASCE Managing Editor. The manuscript for this paper was submitted for review and possible publication on March 1, 2004; approved on June 7, 2006. This paper is part of the *Journal of Structural Engineering*, Vol. 133, No. 1, January 1, 2007. ©ASCE, ISSN 0733-9445/2007/1-96-104/\$25.00.



unit: mm

Fig. 1. Test setup

the ultimate concrete shear strength in the connection is low if the steel beam is not encased in concrete.

In this paper, the writers examine the cyclic behavior of two exterior SRC moment connections with different details. Continuity plates were eliminated in Specimen 1 and a reduced amount of transverse reinforcement than that required by the ACI 318 (1995) was used. Instead of using transverse reinforcement, a steel jacket plate was provided in Specimen 2 to confine the concrete, and the shear capacity of the jacket plate was mobilized by extending continuity plates from the column web to the jacket plate. Both the NEHRP Seismic Provisions (1997) and the AIJ (1987) standards were also evaluated for the prediction of connection shear strength. A comparison of the cyclic behavior between interior and exterior SRC moment connections has been reported elsewhere (Chou and Uang 2002).

## Objectives

The first objective of the study was to examine the effects of two factors on the concrete shear strength in the connection region:

continuity plates and the amount of transverse reinforcement. The second objective was to develop an analytical procedure to quantify the connection shear force developed in concrete.

## Test Specimens

Two full-scale specimens representing an exterior moment connection on the third floor of a seven-story frame were tested (Chou and Uang 2001). The overall dimensions of the specimens and the test setup are shown in Fig. 1. Since the reduced beam section (RBS) has been shown to be effective in lowering both the tensile force in the welded joints and the shear force in the connection region (Engelhardt et al. 1998) for steel construction, this approach is also attractive for composite moment frames for its potential to simplify the connection detailing and design. In this study, RBS with a 50% flange cut-out was used, leading to a 23% reduction of the plastic moment of the beam. A572 Grade 345 (50) steel was used for the steel columns (W12×58) and beams (W24×76), and ASTM A 706M steel was specified for the trans-

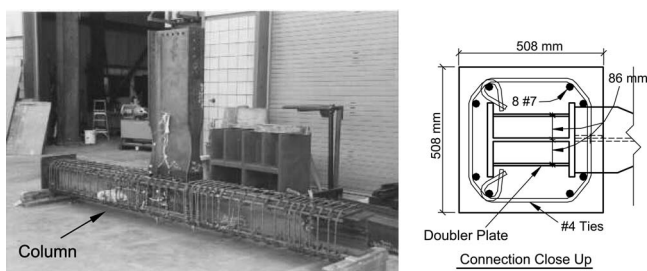


Fig. 2. Specimen 1 overall view prior to concrete encasement

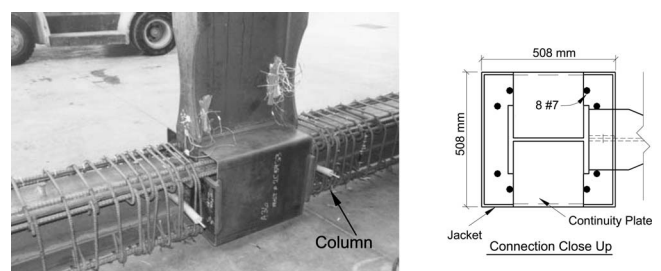


Fig. 3. Specimen 2 overall view prior to concrete encasement

**Table 1.** Specimen Connection Details

Specimen number	SRC column (mm × mm)	Longitudinal bar	Transverse bar	Doubler plate (mm)	Jacket plate (mm)	Continuity plate (mm)
1	508 × 508	8-#7	5-#4	9.5 (Gr. 50)	—	—
2	508 × 508	8-#7	—	—	9.5 (A36)	19 (Gr. 50)

verse and longitudinal reinforcements. The specified 28 day concrete strength,  $f'_{cn}$ , was 35 MPa.

Figs. 2 and 3 show the overall view of the specimens before the steel column was encased in concrete. Table 1 provides additional information of the specimens. Note that the width-thickness ratio ( $b_{cf}/2t_{cf}=7.8$ ) of the steel column section exceeded the limiting width-thickness ratio ( $52/\sqrt{F_{cy}}=7.35$ ) required for steel special moment frame design. This light section was selected to demonstrate the benefit of concrete encasement in preventing local buckling of the steel column.

The connection shear force demand,  $V_{ju}$ , in Table 2 was determined from

$$V_{ju} = \frac{\sum M_b}{0.95d_b} - V_{col} \quad (1)$$

where  $\sum M_b$  is the summation of the beam maximum moment at the face of the SRC column, which is determined by projecting the expected beam moment capacity ( $=1.1Z_{RBS}F_{ye}$ ) at the center of RBS (AISC 1997). The nominal shear strength,  $R_{jn}$ , of the connection was calculated as the summation of the nominal strengths of the structural steel and reinforced concrete shear components, which were determined in accordance with Sec. 9.3 of the AISC Seismic Provisions (1997) and Sec. 21.5 of the ACI 318 (1995), respectively. The strength reduction factor,  $\phi_v$ , of 0.75 and 0.8 was used in calculating the design strength of the structural steel (Sec. 9.3 in AISC 1997) and reinforced concrete (Appendix C in ACI 318 1995), respectively.

### Specimen 1 Connection Design

Specimen 1 used a pair of 9.5 mm (3/8 in.) doubler plates placed away from the column web and five layers of No. 4 transverse reinforcement placed in the connection region (Fig. 2). Table 2 lists the nominal shear strengths of the steel web,  $R_{sw}$ , and the doubler plates,  $R_{sd}$ ; see Chou and Uang (2002) for the calculations of these two quantities.

Because the steel column flange width was less than half the SRC column width, the requirement that the confining member at the connection region be at least three-fourths the column width (Sec. 21.5.2 in ACI 318 1995) is violated. Considering that the steel shape in an SRC column can carry part of the axial load and that less longitudinal reinforcement than that in a similar-sized reinforced concrete column is required, the following equations,

which were modified from Sec. 21.4.4.1 of ACI 318 (1995), were used in this study to design the transverse reinforcement in the connection

$$A_{sh} = 0.3 \frac{sh_c f'_{cn}}{f_{yh}} \left( \frac{A_g}{A_{ch}} - 1 \right) \left( 1 - \frac{F_{cy} A_s}{P_{nc}} \right) \quad (2)$$

$$A_{sh} = 0.09 \frac{sh_c f'_{cn}}{f_{yh}} \left( 1 - \frac{F_{cy} A_s}{P_{nc}} \right) \quad (3)$$

The minimum required area of transverse reinforcement was calculated to be 62% of that required by the AISC Seismic Provisions (1997). This reduction was beneficial for enhancing the constructability. The shear strength provided by the transverse reinforcement in the connection region was calculated based on (ASCE Task Committee 1994)

$$R_{st} = 0.9(2A_{st}f_{yh}N) \quad (4)$$

where  $N$  ( $=5$ )=number of layers of transverse reinforcement. Since the amount of transverse reinforcement was much less than that specified in ACI 318 (1995) and no continuity plates were provided, sufficient confinement to the concrete was not provided in the connection. Thus, the concrete contribution,  $R_c$ , was ignored in the calculation of the connection strength.

### Specimen 2 Connection Design

Specimen 2, shown in Fig. 3, used a 9.5 mm (3/8 in.) steel jacket plate with no transverse reinforcement in the connection region. To mobilize the shear resistance of the steel jacket, continuity plates matching the beam flange thickness were extended from the steel column to the steel jacket. The nominal shear strength of the steel web,  $R_{sw}$ , in Table 2 was computed in the same way as that in Specimen 1. When a steel jacket plate was welded to the transverse and longitudinal beams, Sakaguchi et al. (1988) found that the distribution of shear stress across the width of the jacket plate was parabolic. Based on this finding, the shear strength of the jacket plate was calculated as

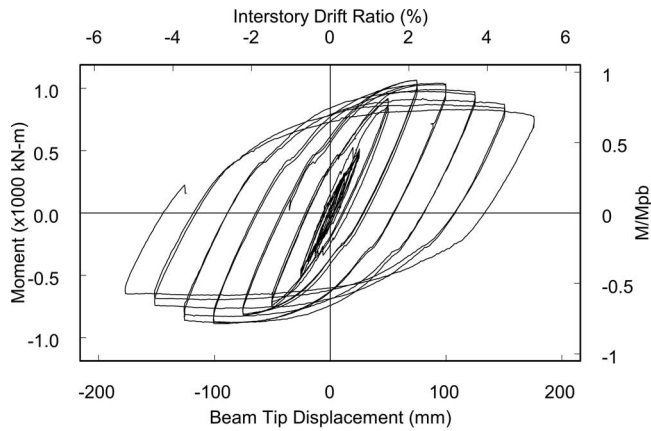
$$R_{sj} = 0.6F_{jy} \left( \frac{5}{6}d_t \right) (2t_j) \quad (5)$$

To avoid shear buckling of the jacket plate, the minimum thickness was set equal to 9.5 mm (3/8 in.), satisfying

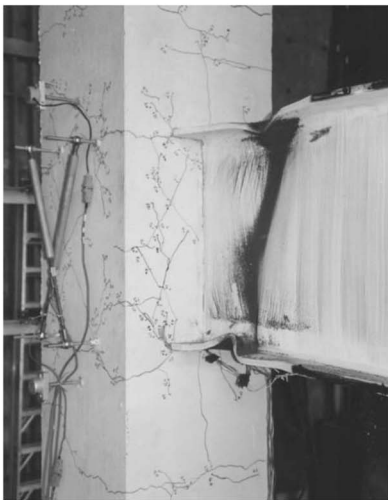
**Table 2.** Components of Connection Shear Strength

Specimen number	$R_{sw}$ (kN)	$R_{sd}$ (kN)	$R_{sj}$ (kN)	$R_{st}$ (kN)	$R_c$ (kN)	$R_{jn}$ (kN)	$R_{jd}$ (kN)	$V_{ju}$ (kN)
1	654	1090	—	481	0	2278	1693	1375
2	654	—	1202	—	182	2038	1538	1375

Note: ( $R_{jd} = \phi_v R_{jn}$ ,  $M_{pb} = 1130$  kN-m,  $M_b = 954$  kN-m).



(a) Moment versus Beam Tip Displacement



(b) Beam Buckling and Concrete Crack Pattern

**Fig. 4.** Specimen 1 global responses and observed performance

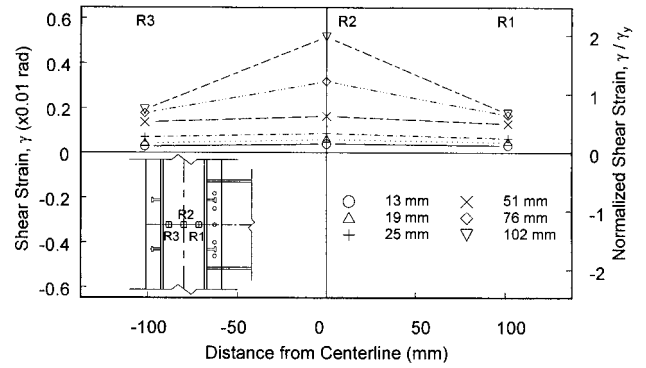
$$t \geq \frac{(d_z + w_z)}{90} \quad (6)$$

According to research conducted by Wakabayashi et al. (1973) as well as Minami and Nishimura (1980), concrete within the steel column flanges and continuity plates could be mobilized for shear resistance. Since the shear strength of the steel column web and jacket plates alone were higher than the required shear strength, the damage in the connection concrete was expected to be minor. Without considering the axial load effect, the concrete shear strength, listed in Table 2, was computed based on  $0.3\sqrt{f'_{cr}}A_{eff}$  (ACI-ASCE 352, 1976). The effective area,  $A_{eff}$ , was computed as

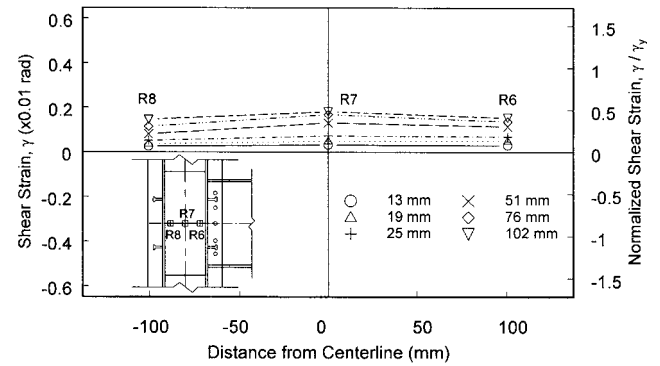
$$A_{eff} = \left( \frac{b_{cf} + b_t}{2} \right) d_t - A_s \quad (7)$$

### Experimental Results

Each specimen was tested cyclically by imposing a pre-defined displacement history to the end of the beam. The displacement history followed that recommended by ATC-24 (1992) for the



(a) Column Web



(b) Doubler Plate

**Fig. 5.** Specimen 1 column web and doubler plate shear strain profiles

cyclic testing of components. The concrete compressive strength,  $f'_c$ , at the day of testing for Specimens 1 and 2 were 43 and 41 MPa, respectively.

For Specimen 1, the relationship between the beam tip displacement and the moment computed at the face of the SRC column is shown in Fig. 4(a). The interstory drift ratio was computed by dividing the beam tip displacement by the beam centerline span. The moment was also normalized by the nominal plastic moment,  $M_{pb}$ , of the full beam section. The test was stopped after significant buckling of the beam [Fig. 4(b)] occurred at 5.2% interstory drift.

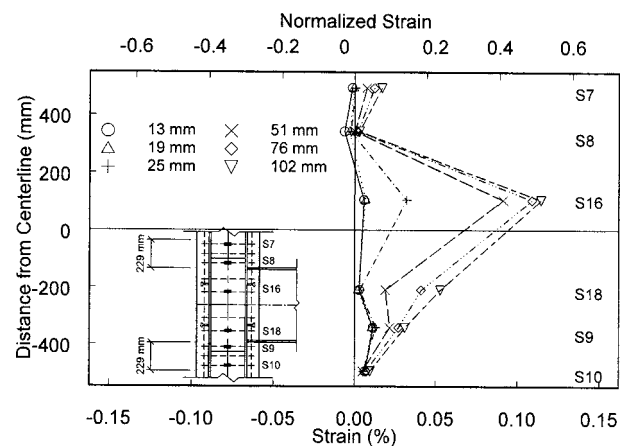
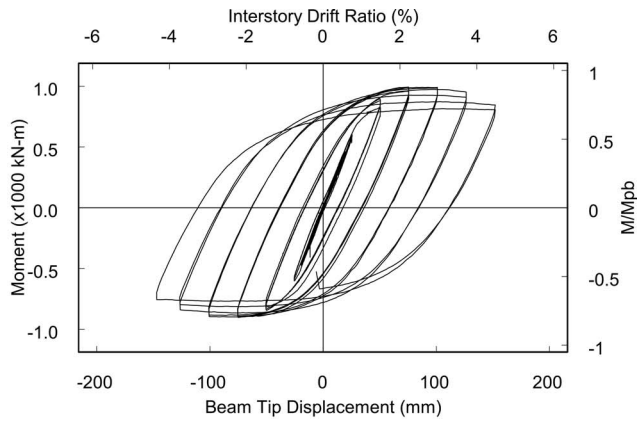
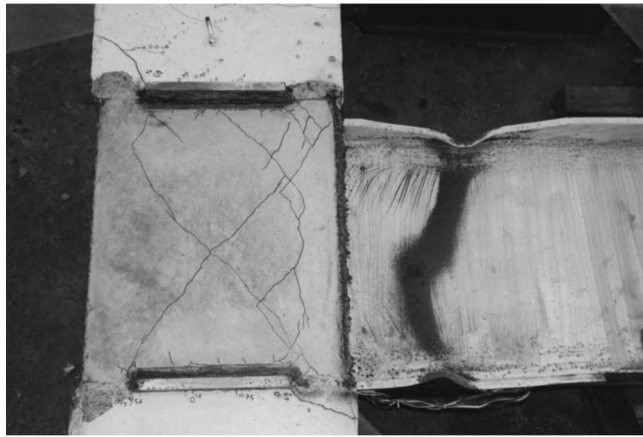


**Fig. 6.** Specimen 1 transverse reinforcement strain profiles



(a) Moment versus Beam Tip Displacement



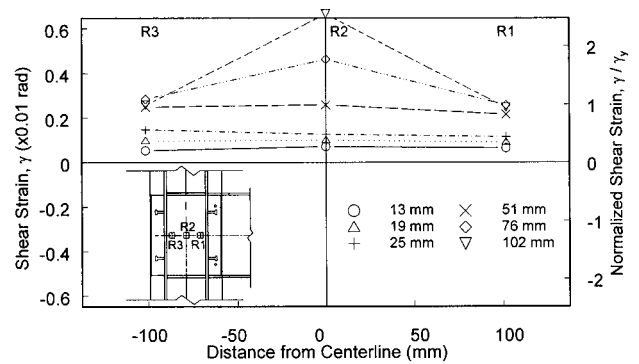
(b) Connection Concrete Crack Pattern

**Fig. 7.** Specimen 2 global responses and observed concrete cracking

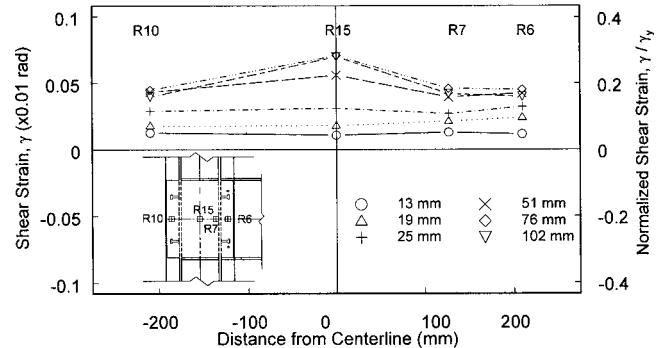
Shear strain profiles in the steel column web are shown in Fig. 5(a); shear strain in the center location reached  $2\gamma_y$  at a beam tip displacement of 102 mm (3.0% interstory drift). Shear strain profiles in one doubler plate [Fig. 5(b)] show less shear deformation. Strain gage measurements indicated that transverse reinforcement in the connection remained in the elastic range (Fig. 6), and the beam web that was embedded in the concrete portion helped resist part of the connection shear.

For Specimen 2, the maximum interstory drift reached more than 4% [Fig. 7(a)] before the beam top flange at the reduced beam section fractured due to low-cycle fatigue. The jacket plate was removed after the test in order to examine the concrete crack pattern in the connection region. Fig. 7(b) shows two diagonal shear cracks between the steel column flanges, which indicates that the concrete within the steel column flanges and continuity plates was mobilized for shear resistance.

Fig. 8(a) shows that shear strain profiles in the steel column web were similar to those observed in Fig. 5(a). Fig. 8(b) depicts shear strain profiles across the jacket plate width, indicating less shear deformations than those in the doubler plates [Fig. 5(b)]. The profiles also show that the shear strain was relatively uniform across the plate width. Fig. 9 shows the measured strains on the north and south sides of the jacket. The hysteresis loops in the figure were similar to those of the transverse reinforcement of Specimen 1 (Chou and Uang 2001); therefore, the jacket plate



(a) Column Web



(b) Jacket Plate

**Fig. 8.** Specimen 2 column web and jacket plate shear strain profiles

was effective in providing confinement to the concrete in the connection region.

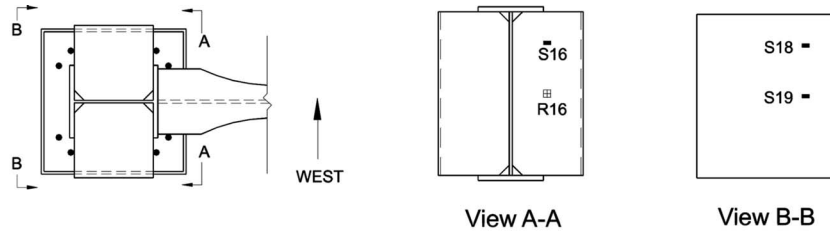
### Connection Shear Strength

Figs. 10(a and b) show the distribution of shear forces in the connection for Specimens 1 and 2, respectively. Shear force of each component was computed from the strain gage readings and the associated plate or transverse reinforcement area. The strains were assumed to be linear between the measured strain locations in a plate. The post-yield shear modulus of the steel column web was assumed to be  $0.045G$  (Krawinkler 1978). The shear force developed in concrete,  $V_c$ , was obtained by subtracting the contribution of each steel component from the total connection shear. At higher displacement amplitudes, it is observed that the column web and doubler plates were very effective in resisting a significant amount of shear in Specimen 1. Nevertheless, the concrete component was reduced from half the total shear force to almost zero as the deformation level was increased. But for Specimen 2, the concrete still resisted 30% of the connection shear at higher deformation levels.

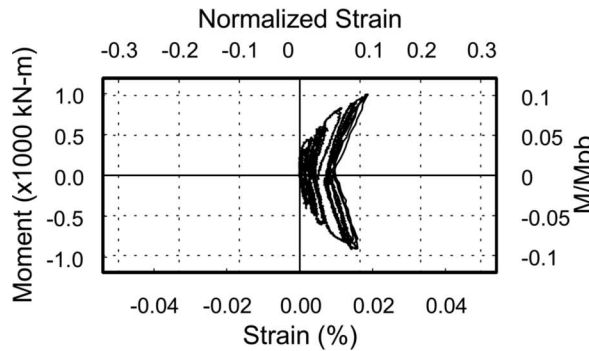
In order to compare the concrete shear strength obtained from the test with those predicted by ACI-ASCE 352 (1976), NEHRP provisions (1997), and AIJ Standards (1987), the average shear stress,  $\tau_c$ , of the concrete was computed as

$$\tau_c = \frac{V_c}{A_{\text{eff}}} \quad (8)$$

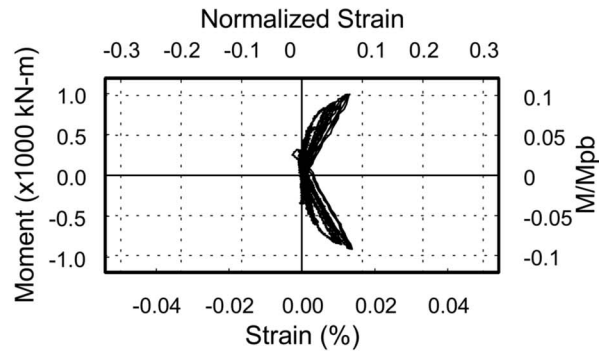
where  $A_{\text{eff}}$  is the effective area [Eq. (7)]. The average shear stress,  $\tau_c$ , for both the concrete and transverse reinforcement was



(a) Rosette and Strain Gage Locations



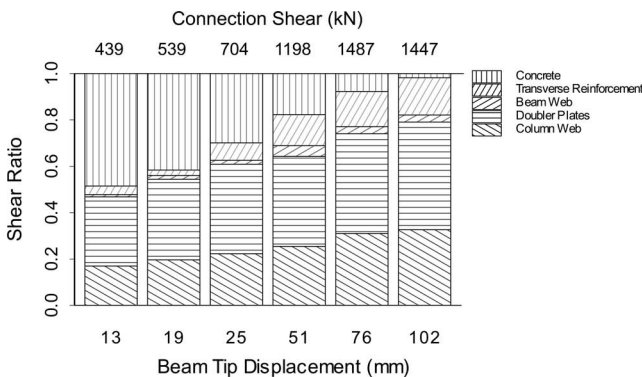
(b) Rosette R16-1



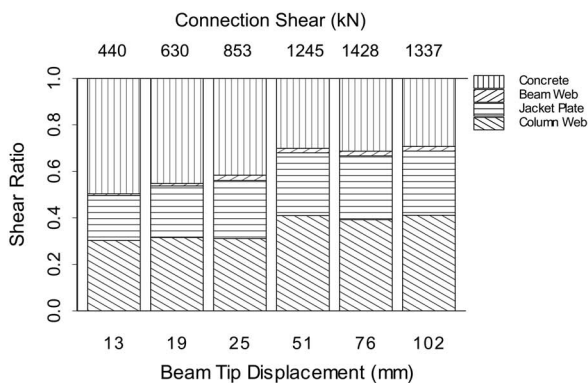
(c) Strain Gage S19

Fig. 9. Specimen 2 measured jacket plate strains on the north and south sides

$$\tau_{ct} = \frac{V_c + V_{st}}{A_{eff}} \quad (9)$$



(a) Specimen 1



(b) Specimen 2

Fig. 10. Distribution of shear forces in connection region

The variations of  $\tau_c$  and  $\tau_{ct}$  with respect to the beam tip displacement are shown in Fig. 11. The maximum applied load was reached at a beam tip displacement of 76 mm (2.2% interstory drift), and the shear could not increase further due to beam buckling. The maximum  $\tau_c$  values for Specimens 1 and 2 were  $0.19\sqrt{f'_c}$  and  $0.4\sqrt{f'_c}$ , respectively, less than the strength ( $1.02\sqrt{f'_c}$ ) specified in the AIJ Standards (1987). Note that the AIJ Standards (1987) was developed mainly based on the research work of Wakabayashi et al. (1973) as well as Minami and Nishimura (1980), which included continuity plates but not transverse reinforcement in the connection.

The concrete strength for Specimen 1 started to degrade before the maximum applied load was reached, but the transverse reinforcement was still in the elastic range (Fig. 6). The value of

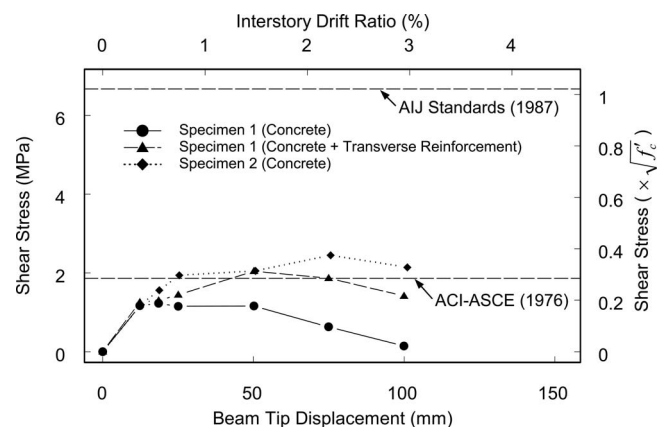
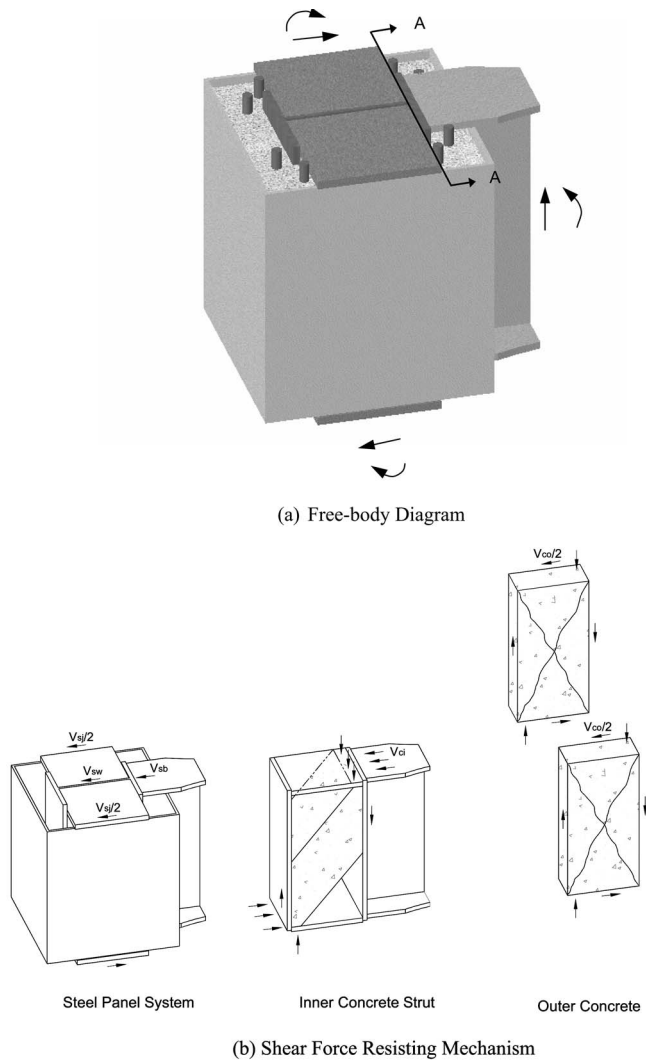


Fig. 11. Shear stress in concrete



**Fig. 12.** Specimen 2 shear-resisting mechanism

$\tau_{ci}$  reached  $0.32\sqrt{f'_c}$ , which is less than that ( $1.0\sqrt{f'_c}$ ) specified in Sec. 21.5.2 of the ACI 318 (1995). The maximum concrete shear resistance,  $\tau_c$ , for Specimen 1 degraded before reaching the strength ( $0.3\sqrt{f'_c}$ ) specified in ACI-ASCE 352 (1976), but that of Specimen 2 exceeded this specified strength. This behavior can be attributed to the effect of the continuity plate. It would be unconservative to use  $0.3\sqrt{f'_c}$  to estimate the concrete shear resistance for the exterior SRC moment connection without using the continuity plate. The ultimate shear strength of the concrete for Specimen 2 was not reached due to strength degradation and, ultimately, the fracture of the beam. An analytical model for predicting the shear force developed in concrete of Specimen 2 is presented next.

### Analytical Model for Concrete Shear Resistance

Shown in Fig. 12 is the free body of the connection and the associated shear-resisting mechanisms. The connection shear-resisting mechanism is composed of a steel panel system, an inner concrete strut, and an outer concrete panel. The steel panel system consists of the steel column web, steel jacket plate, and beam web embedded in the SRC column. The connection shear can be trans-

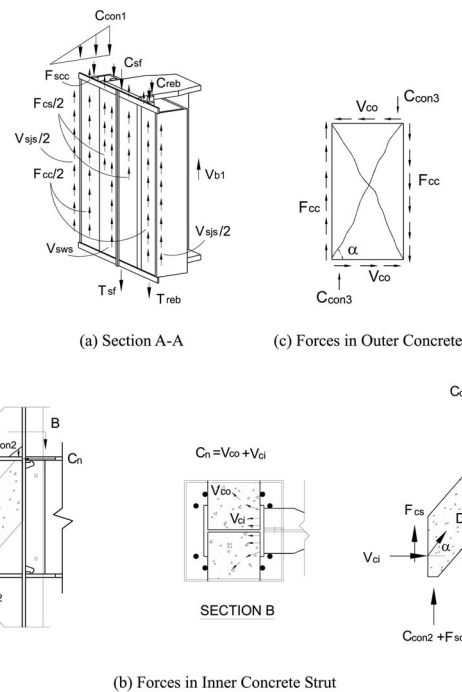


**Fig. 13.** Specimen 2 force transfer mechanism

ferred to the steel jacket through the top and bottom continuity plates. The shear force developed in each component of the steel panel system ( $V_{sw}$ ,  $V_{sj}$ , and  $V_{sb}$  for column web, jacket, and beam web, respectively) can be computed directly from the measured shear strain and the associated plate areas. The inner concrete strut within the steel column flanges and continuity plates can be mobilized to resist a shear of  $V_{ci}$ . The outer concrete contribution to the connection shear is denoted as  $V_{co}$ . The shear force transfer mechanism is identified as follows.

The section view in Fig. 13(a) is obtained by cutting through the steel column at Sec. A-A in Fig. 12(a). Assuming strain compatibility between the concrete and steel above and below the connection, all flexural forces ( $T_{reb}$ ,  $T_{sf}$ ,  $C_{con1}$ ,  $C_{sf}$ , and  $C_{reb}$ ) in Fig. 13(a) are computed from a moment-curvature analysis program (Bentz and Collins 2000) at different load steps.  $V_{sws}$  and  $V_{sj}$  in Fig. 13(a) represent the vertical connection shear in the column web and jacket plates, respectively, and are converted from the horizontal shears  $V_{sw}$  and  $V_{sj}$  in Fig. 12(b) as follows:

$$V_{sws} = \frac{V_{sw}(d_b - 2t_{bf})}{(d_c - 2t_{cf})} \quad (10)$$

$$V_{sj} = \frac{V_{sj}(d_b - 2t_{bf})}{\frac{5}{6}(d_t - 2t_j)} \quad (11)$$

Considering force equilibrium [Eq. (12)] in the vertical direction of Fig. 13(a), three remaining unknowns are: (1)  $F_{cs}$ , the friction force between the steel column flange and inner concrete, (2)  $F_{cc}$ , the friction force in the concrete outside the steel flange, and (3)  $F_{scc}$ , the force in the continuity plate

$$F_{scc} + F_{cc} = (T_{reb} + T_{sf} + C_{con1} + C_{sf} + C_{reb}) - (V_{sws} + V_{sj} + V_{b1}) - F_{cs} \quad (12)$$

The horizontal bearing force,  $C_n$ , which creates a friction force  $F_{cs}$  in the vertical direction, is calculated as

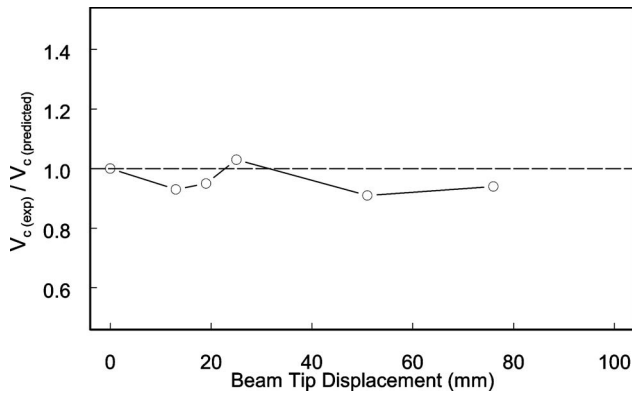


**Fig. 14.** Ratios between experimental and predicted concrete shear force

$$C_n = V_{ju} - V_{sw} - V_{sj} - V_{sb} = V_{ci} + V_{co} \quad (13)$$

This force is also transferred to the other side of the steel column through the continuity plate [Fig. 13(b)]. The friction force  $F_{cs}$  is calculated as the bearing force,  $C_n$ , times the shear friction coefficient,  $\lambda$ . Mattock and Hawkins (1972) reported that the externally applied compressive force acting transversely to the shear plane of the concrete is additive to the clamping force if it exists. This is also accepted in Sec. 11.7.7 of ACI 318 (1995). The friction force,  $F_{cs}$ , developed in the SRC connection is thus computed as

$$F_{cs} = C_n \lambda \quad (14)$$

where  $\lambda=0.7$ . The inner concrete strut in Fig. 13(b), is

$$V_{ci} = \frac{F_{cs} + C_{con2} + F_{scc}}{\tan \alpha} \quad (15)$$

where the angle  $\alpha(=58^\circ)$  is calculated as

$$\alpha = \tan^{-1} \left( \frac{0.75d_b}{d_c - 2t_{cf}} \right) \quad (16)$$

and  $C_{con2}$ =flexural force in the SRC column obtained from the moment-curvature analysis.

The outer concrete contribution, shown in Fig. 13(c), is estimated as

$$V_{co} = \frac{F_{cc} + C_{con3}}{\tan \alpha} \quad (17)$$

where  $C_{con3}$ , the flexural force in the SRC column, is obtained from the moment-curvature analysis. The predicted concrete contribution (including the inner concrete strut and outer concrete panel) is computed as the summation of Eqs. (15) and (17)

$$V_c = V_{ci} + V_{co} = \frac{F_{cs} + C_{con2} + C_{con3} + F_{scc} + F_{cc}}{\tan \alpha} \quad (18)$$

where  $F_{scc}$  and  $F_{cc}$  are obtained from Eq. (12), and  $F_{cs}$  is obtained from Eq. (14). A comparison of the predicted and experimental shear force developed in concrete shows a good correlation up to the drift level tested (Fig. 14).

## Conclusions

Two exterior SRC moment connection details that aim to enhance the constructability of a type of special composite moment resisting frames with steel-encased reinforced concrete (SRC) columns and steel beams were proposed and tested. This paper evaluates the effects of continuity plate and transverse reinforcement on concrete shear resistance. Specimen 1 used about 40% less transverse reinforcement than that required by the ACI 318 (1995), and a pair of doubler plates was added in the connection; continuity plates were eliminated. Specimen 2 used a steel jacket plate to surround the connection and continuity plates were added; no transverse reinforcement was used.

Although transverse reinforcement in the connection of Specimen 1 remained in the elastic range (Fig. 6), concrete degraded in resisting shear before the maximum beam load was reached [Fig. 10(a)]. The jacket plate in Specimen 2 was effective in resisting shear [Fig. 10(b)] in addition to providing confinement in the connection region (Fig. 9). No strength degradation of the concrete was noted before the maximum applied load was reached (Fig. 11).

To mobilize the shear resistance of the concrete in the connection region, continuity plates are needed for the formation of a compression strut. An analytical model was proposed to predict the shear force developed in concrete. When continuity plates were not used in the exterior SRC moment connection, this study showed that concrete shear resistance cannot be counted on. This study also showed that such resistance is not sensitive to the amount of transverse reinforcement used.

## Acknowledgments

This research project was sponsored by National Science Foundation (Award No. CMS-9632498) with Dr. Shih-Chi Liu as the Program Director. Mr. Ali Sadre and Professor Keh-Chyuan Tsai provided technical advice throughout the testing program.

## Notations

The following symbols are used in this paper:

- $A_{ch}$  = area of SRC column measured out-to-out of transverse reinforcement;
- $A_{eff}$  = effective shear area;
- $A_g$  = area of SRC column;
- $A_s$  = area of steel column;
- $A_{sh}$  = area of transverse reinforcement required;
- $A_{st}$  = area of transverse reinforcement provided;
- $b_{cf}$  = width of steel column flange;
- $b_t$  = width of SRC column;
- $C_{con1}$  = flexural compression force in concrete;
- $C_{con2}$  = flexural compression force in concrete within steel column flanges;
- $C_{con3}$  = flexural compression force in an outer concrete panel;
- $C_n$  = bearing force;
- $C_{reb}$  = flexural compression force in longitudinal reinforcement;
- $C_{sf}$  = flexural compression force in steel column flange;
- $d_b$  = depth of steel beam;
- $d_c$  = depth of steel column;
- $d_i$  = depth of SRC column;



$d_z$  = depth of steel panel zone;  
 $F_{cc}$  = friction force in concrete outside the steel flange but along Sec. A-A;  
 $F_{cs}$  = friction force between steel column flange and inner concrete;  
 $F_{cy}$  = specified yield strength of steel column web;  
 $F_{jy}$  = yield strength of steel jacket plate;  
 $F_{sc}$  = force in continuity plate;  
 $F_{ye}$  = expected yield strength;  
 $f_c^t$  = concrete testing strength;  
 $f_{cn}^t$  = specified concrete strength;  
 $f_{yh}$  = specified yield strength of transverse reinforcement;  
 $G$  = elastic shear modulus of steel;  
 $h_c$  = dimension of column core measured center-to-center of confining reinforcement;  
 $M_b$  = beam maximum moment at the face of the SRC column;  
 $M_{pb}$  = beam plastic moment of full section;  
 $N$  = number of transverse reinforcement;  
 $P_{nc}$  = nominal axial compressive strength of SRC column;  
 $R_c$  = nominal shear strength in concrete;  
 $R_{jn}$  = nominal shear strength in SRC connection;  
 $R_{jd}$  = design shear strength in SRC connection;  
 $R_{sd}$  = nominal shear strength in steel double plate;  
 $R_{sj}$  = nominal shear strength in steel jacket plate;  
 $R_{sw}$  = nominal shear strength in steel column web;  
 $R_{st}$  = nominal tensile strength in transverse reinforcement;  
 $s$  = spacing of transverse reinforcement;  
 $T_{sf}$  = flexural tension force in steel column flange;  
 $T_{reb}$  = flexural tension force in longitudinal reinforcement;  
 $t_{cf}$  = thickness of steel column flange;  
 $t_j$  = thickness of jacket plate;  
 $V_{b1}$  = beam shear;  
 $V_c$  = shear force developed in concrete ( $=V_{ci}+V_{co}$ );  
 $V_{ci}$  = shear force developed in inner concrete strut;  
 $V_{co}$  = shear force developed in outer concrete;  
 $V_{col}$  = column shear demand;  
 $V_{ju}$  = connection shear demand;  
 $V_{sb}$  = shear force developed in steel beam web;  
 $V_{sj}$  = shear force developed in jacket plates;  
 $V_{sjs}$  = vertical connection shear in steel jacket plates;  
 $V_{st}$  = shear force developed in transverse reinforcement;  
 $V_{sw}$  = shear force developed in steel column web;  
 $V_{sws}$  = vertical connection shear in steel column web;  
 $w_z$  = width of steel panel zone;  
 $Z_{RBS}$  = plastic modulus at RBS section;  
 $\alpha$  = angle of diagonal concrete crack;  
 $\lambda$  = friction coefficient;  
 $\gamma$  = steel shear strain;  
 $\gamma_y$  = steel shear yield strain;  
 $\tau_c$  = shear stress of concrete on effective area;  
 $\tau_{ct}$  = shear stress of concrete and transverse reinforcement on effective area;  
 $\phi_v$  = shear strength reduction factor; and  
 $\Sigma M_b$  = summation of beam maximum moment at face of SRC column.

## References

American Concrete Institute-American Society of Civil Engineers (ACI-ASCE), Connection Committee 352. (1976). "Recommendations for

design of beam-column connections in monolithic reinforced concrete structures." *ACI J.*, 73(7), 375–393.

American Concrete Institute (ACI). (1995). "Building code requirements for structural concrete (*ACI 318-95*) and commentary (*ACI 318R-95*)." American Concrete Institute, Farmington Hills, Mich.

American Institute of Steel Construction (AISC). (1997). *Seismic provisions for structural steel buildings*, American Institute of Steel Construction, Chicago.

American Society of Civil Engineers (ASCE) Task Committee. (1994). "Guidelines for design of joints between steel beams and reinforced concrete columns." *J. Struct. Eng.*, 120(8), 2330–2357.

Applied Technology Council (ATC). (1992). "Guidelines for cyclic seismic testing of components of steel structure for buildings." *Rep. No. ATC-24*, Applied Technology Council, Redwood City, Calif.

Architectural Institute of Japan (AIJ). (1987). *Standards for structural calculation of steel reinforced concrete structures*, Architectural Institute of Japan.

Architectural Institute of Japan (AIJ). (1994). *Design guidelines for composite RCS connections*, Architectural Institute of Japan.

Bentz, E. C., and Collins, M. P. (2000). "Moment-curvature analysis program response." Dept. of Civil Engineering, Univ. of Toronto, Canada.

Chou, C. C., and Uang, C. M. (2001). "Experimental and analytical studies of two types of moment connections for composite special moment frames." *Rep. No. SSRP 98-12*, Dept. of Structural Engineering, Univ. of California, San Diego.

Chou, C. C., and Uang, C. M. (2002). "Cyclic performance of a type of steel beam to steel-encased reinforced concrete column moment connection." *J. Constr. Steel Res.*, 58, 637–663.

Deierlein, G. G. (1988). "Design of moment connections for composite framed structures." Doctoral thesis, Dept. of Civil Engineering, Univ. of Texas, Austin, Tex.

Engelhardt, M. D., Winneberger, T., Zekany, A. J., and Potyraj, T. J. (1998). "Experimental investigation of dogbone moment connections." *Eng. J.*, 35(4), 128–139.

FEMA. (1997). "Recommended provisions for the development of seismic regulations for new buildings." *FEMA-222A*, National Earthquake Hazards Reduction Program, Washington, D. C.

Izaki, Y., Yamanouchi, H., Nishiyama, I., and Fukuchi, Y. (1988). "Seismic behavior of girder-to-column connections developed for an advanced mixed structure system." *Proc., 9th World Conf. on Earthquake Eng., IV*, Tokyo-Kyoto, Japan, 707–712.

Kanno, R. (1993). "Strength, deformation, and seismic resistance of connections between steel beams and reinforced concrete columns." Doctoral thesis, School of Civil and Environmental Engineering, Cornell Univ., Ithaca, NY.

Krawinkler, H. (1978). "Shear in beam-column joints in seismic design of steel frames." *Eng. J.*, 15(3), 82–91.

Kuramoto, H. (1996). "Seismic resistance of through column type connections for composite RCS systems." *Proc., 11th World Conf. on Earthquake Eng., 1755-1762*.

Mattock, A. H., and Hawkins, N. M. (1972). "Shear transfer in reinforced concrete-recent research." *PCI J.*, 17(2), 20–39.

Minami, K., and Nishimura, Y. (1980). "Hysteretic characteristics of beam-to-column connections in steel reinforced concrete structures." *Proc., 7th World Conf. on Earthquake Eng., II*, 305–308.

Sakaguchi, N., Tominaga, H., Murai, Y., Takase, Y., and Shuto, K. (1988). "Strength and ductility of steel beam-RC column connection." *Proc., 9th World Conf. on Earthquake Eng., IV*, Tokyo-Kyoto, Japan, 713–718.

Sheikh, T. M. (1987). "Moment connections between steel beams and concrete columns." Doctoral thesis, Dept. of Civil Engineering, Univ. of Texas at Austin, Tex.

Wakabayashi, M., Nakamura, T., and Morino, S. (1973). "An experimental of steel reinforced concrete cruciform frame." *Bulletin of Disaster Prevention Research Institute*, Kyoto Univ., Japan, 23, 75–110.